A Simple Model of Rolling Motion

T. Foster and C. Beaupre

April 27, 2022

Abstract

The perceived rolling motion in the spiral arms in the milky way galaxy is interpreted by Yuan and Wallace (1973) as an apparent motion due to the combined effects of bending of the galactic plane and the differential motion. This study applies the CARS recent 21 cm survey to confirm whether the rolling motion is an apparent effect or not. Gradient measurements use Gaussian curve-fitting on velocity-latitude diagrams in the second quadrant of the milky way galaxy. The combination of bending and differential motion by Yuan and Wallace (1973) must be sufficient in this survey to conclude apparent rolling motion using contour mapping proposed by Feitziner and Spicker (1985). The focus of this study only represents the second quadrant of the Milky Way Galaxy. Several complicating factors described in the theory section elaborate on why the second quadrant is the most reliable measurement. If surmountable evidence of rolling motion occurs in the second quadrant, then the rolling motion should be tested and observed in other quadrants. Differential motion theoretically calculated is compared with gradient measurements to determine if rolling motion exists. A simple model showed that a small rolling motion exists for the Perseus and Cygnus arms.

1 Theory

1.1 Velocity Theory

The spiral arms located in the second quadrant in the CARS survey are the Perseus, Cygnus, and outer arm. The Perseus arm is below the galactic plane, and the Cygnus arm is above the galactic plane. The outer spiral arm is above the galactic plane. Measurements of the outer arm are inconclusive due to the relative size of the arm and minimal velocity-latitude points attainable. The velocity-latitude gradients of each spiral arm are generally uniform and occur at a considerable negative velocity. The spiral arms are centroids shifted from the galactic plane allowing for measurements of each spiral arm. The Perseus and Cygnus arms have drastic changes in negative velocity with respect to longitude. In the second quadrant, the Perseus and Cygnus arms will shift from $-0.7 * 10^5$ m/s to 0 m/s. The outer arm velocity hovers around $-1 * 10^5$ m/s. The position of the spiral arm determines the sign and magnitude of the

spiral arm. Tangential velocity is negative when the centroid moves towards us and positive moving away. We expect to see negative tangential velocity in the second quadrant.

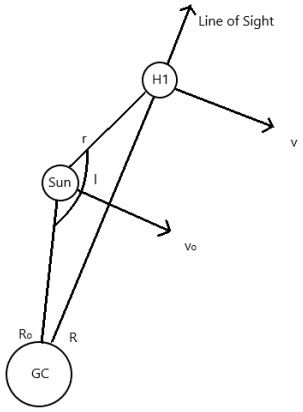

Figure 1: An illustration of a planar diagram measuring the velocity along the line of sight from the galactic center.

Using the trigonometric equation, we derive the equation for the velocity along the line of sight. The distance from the galactic center (R) to the hydrogen cloud is derived using cosine law from 1. Parameters needed to calculate the distance from the galactic center include the solar galactocentric radius (R_o), the distance from the sun to the hydrogen cloud (r), the longitude (l) and latitude (b).

$$R = \sqrt{((R_o)^2 + R^2 * cos(b)^2 - 2R_o * r * cos(l) * cos(b))}$$

The distance from the galactic center (R) to the hydrogen cloud is derived using the cosine law.

$$v_l = R_o * (\frac{v}{R} - \frac{v_o}{R_o}) * sin(l)$$

The planar line of sight tangential velocity for a flat galactic disk.

$$v_l = R_o * (\frac{v}{R} - \frac{v_o}{R_o}) * sin(l) * cos(b)$$

The non-planar line of sight velocity.

The non-planar tangential velocity equation determines the theoretical velocity along the line of sight. The parameters needed to calculate the distance from the galactic center include the solar galactocentric radius (R_o), the distance from the galactic center to the hydrogen cloud (R), the longitude (l), and latitude (b), and velocity of the hydrogen cloud (v). The velocity calculation

uses longitude and latitude parameters corresponding to the velocity-latitude measurements of the CARS survey.

Warping occurs in disk galaxies and is necessary for our understanding of the milky way galaxy's structure. Figure 2 shows the spiral arms in the deviation from the galactic center. The velocity deviation in figure 2 demonstrates the longitude range of the Perseus and Cygnus arms. Perseus and Cygnus arm measurements were acquired over the full range of longitudes in the second quadrant to determine if rolling motion exists.

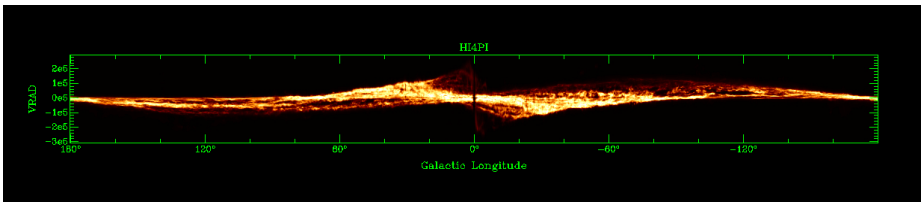

Figure 2: This figure is a visual representation of the CARS survey across all quadrants.

Velocity-latitude gradients are measured using the latitude-velocity diagram for a range of specific longitudes. The theoretical gradient sign depends on the line-of-sight velocity with respect across the spiral arm and whether the axis of symmetry of the cross-section of the spiral arm passes above or below the sun (Yuan and Wallace, 1973). In the second quadrant, negative gradients should occur. Gradient sign and magnitude of the velocity-latitude diagrams across a range of longitudes are measured.

1.2 Contour Mapping

Tangential velocities measured using contour maps determine the relative distance to the H1 cloud along a line of sight. The magnitude will increase with respect to the radius from the galactic center. The vertical latitude offset of the spiral arms occurs from the warping of the galactic plane. The Perseus and Cygnus arms are offset vertically from the galactic center. The velocity-latitude range of the Perseus and Cygnus arm would overlap if there were no vertical offset from the galactic center. Figure 3 visually represents the difference in latitude between the Perseus and Cygnus arms. Contour maps of the spiral arms distinguish the temperature density.

Figure 3 visually represents equal temperature density contours of H1 along a line of sight for a given longitude. Along a line of sight, contour elevations correspond to temperature density. Contour maps were applied to all velocity-latitude maps using a [10,90] percent with intervals of 10 percent of the peak temperature. The application of a contour map to the CARS survey presents the definitive structure of the spiral arms. The equal density contour applied to the velocity-latitude diagram will significantly drop off to a lower percentage value of peak temperature outside the centroid. Linear rolling was measured

using 20 percent and 50 percent of peak contour peak values for a basis of gradient measurements. The four percentage of contour maps applied in Feitziner and Spicker (1985) to their surveys were 15, 30, 50, and 80 percent of peak gradient values. To incorporate Feitziner and Spicker (1985), the differences in the gradient of 15 percent is comparable with a 20 percent peak fit. The 80 percent would not contain enough velocity-latitude pairs to make a conclusive result. The CARS fit contains distinct ridges between the high peak and lower peak values which would have a very similar comparison between 30 and 50 percent. 20 and 50 percent contour maps define the latitude range for velocity measurements. Velocity-latitude pairs of the spiral arm will linearly shift. Figure 3 demonstrates that differential rotation occurs in both spiral arms.

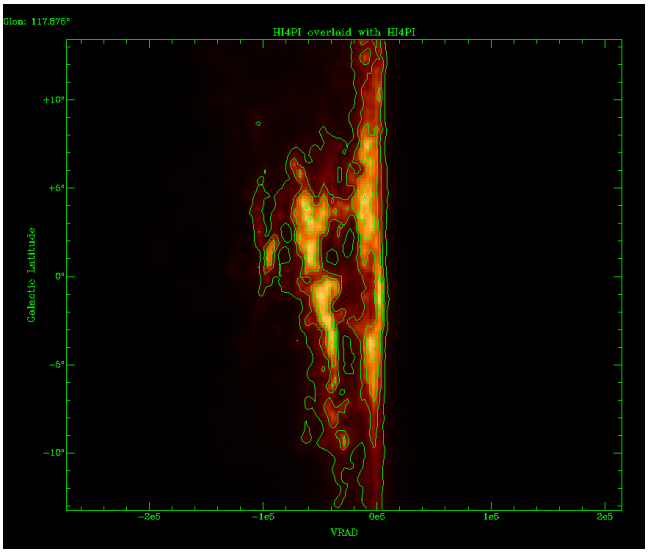

Figure 3: his velocity-latitude diagram demonstrates a contour overlay onto the longitude of 117.875 degrees.

The velocity difference between the lowest and highest latitude spiral arm positions determines the magnitude of the velocity-latitude gradient for a simple model. The bottom latitude position for velocity and latitude uses the symbol (-) and the highest position (+).

$$\frac{dv_l}{db} = (\frac{v_+ - v_-}{b_+ - b_-})$$

The observational velocity along the line of sight at the two extremities of the spiral arm calculates the simple linear model. The theoretical gradient calculation used the lowest and highest measured velocity-latitude position pair. Raising the latitude significantly above the galactic plane will observe outside the milky way galaxy. The 20 percent and 50 percent temperature density contour lens determines the two different latitude parameters for the theoretical

gradient. The gradient from the simple two-point system directly compares with gradient measurements using a linear fit of velocity-latitude pairs across the latitude length of each arm.

The theoretical linear fit method to evaluate the gradient requires a minimum of two velocity-latitude pairs. Two velocity-latitude sets are needed since the theoretical gradient is linear. An increase in velocity-latitude positions across the spiral arm results in greater accuracy. Outer arm gradients were not analyzed since minimal velocity-latitude pairs were attainable. Measurements of the outer arm have scattering and randomness, which would not be sufficient to conclude rolling motion. The latitude range is significantly smaller in the outer arm than in the Perseus and Cygnus arms. A small array would not be able to provide enough velocity-latitude pairs for conclusive gradient analysis. The Perseus and Cygnus arms decrease in latitude length approaching the third quadrant from the second quadrant. The reduced range of the Perseus and Cygnus arms results in lower velocity-latitude pairs. The reduction of velocity-latitude positions results in more scattering and randomness. The linear fits become less accurate with fewer velocity-latitude pairs approaching the third quadrant from the second.

The CARS 21 cm survey of the Milky Way Galaxy contains velocity-latitude diagrams to determine the gradients of rolling motions in the spiral arms. Spiral arm gradient distribution from the galactic plane is linear with low amounts of curvature. The survey gradients obtained across different longitudes with a distribution of H1 in the spiral arms determine rolling motion. The velocity-latitude diagrams with contour density map applications measure velocity across a latitude range for a constant longitude. Measurements of velocity-latitude positions from the overlay of contour maps interpret rolling motion. CARS survey gradient measurements in the second quadrant will either support the differential rolling motion or is an apparent effect.

1.3 Gradient Complications

The apparent rolling motion observed in the spiral arms is handled separately within the second quadrant (Yuan and Wallace, 1973). The first and fourth quadrants are in the interior of the sun's position and contain complications that affect gradient measurement accuracy. The second and third quadrants are exterior of the sun's location and have fewer complications in gradient measurement accuracy. The observable list of obstacles in the interior determines that the second and third quadrants provide the best gradient measurement accuracy. The second and third quadrants should present similar gradient magnitudes with different signs.

Quadrant two is the most resilient to effects complicating the perception of rolling motion for the Perseus and Cygnus arms. Multiple interior complications gradient measurements of rolling motion reduce gradient accuracy. Obstacles observed in the interior are distance ambiguity, the crowding effect, corrugation of the galactic plane, nonuniformity of the spiral arm, and bifurcations of the spiral arms. Each complication causes an increase in uncertainty for the mea-

sured gradients. The focus of this study is within the second quadrant because it is the most resilient to complicating factors.

Distance ambiguity describes the thermal brightness along the line of sight. The temperature along a line of sight can have more than one distinct contribution. The perceived temperature would increase along this line of sight with every contribution. When more than one contribution to the temperature occurred along a line of sight, ambiguity in the distance where we determine that source occurs. Multiple temperatures are observed along the line of sight towards the first and fourth quadrants. The increased likelihood of alignment increase uncertainty in gradient measurements.

The crowding effect explains which gradient measurements will not be used to calculate gradients to prove rolling motion. The crowding effect occurs when the line of sight passes through the spiral arm near one of its tangent points. Hydrogen clouds distributed along this interval centered on the tangent point clusters into the approximate region of velocity. Sufficient crowding occurs near a tangent point which will cause a high amount of uncertainty. The increased overlap of hydrogen along the line of sight close to the tangent point will increase gradient uncertainty.

The ripples in the Milky Way Galaxy represent the corrugation of the galactic plane. An example of corrugation envisioned from a drop of water in a non-moving pool of water with the displacement causing a ripple effect throughout the entire system. Ripples of the spiral arms are observed and occur in the closest proximity to our sun. In the anti center region containing most of the second quadrant, oscillation asymmetry in the main sequence star counts on either side of the galactic plane using the Sloan Digital Sky Survey (Yan Xu, et al., 2015). They showed that the disk is not azimuthally symmetric around the galactic anti-center and that correspondence occurs between observed oscillations and the spiral structure of the milky way galaxy. When a significantly massive object interacts with the milky way galaxy, the galactic center experiences a greater gravitational force than the spiral arms. The difference in gravitational attraction would cause the galactic center in the milky way galaxy to move relative to the spiral arms. The displacement of the galactic center causes the spiral arms to adjust the rotational disk to the new location of the galactic center. The spiral arms adjust to the displacement of the galactic center and oscillate towards their new equilibrium position. The ripples are presumed to occur along the entirety of the milky way galaxy originating from the small displacement of the galactic center. Hydrogen clouds will appear closer to the galactic plane as you increase the relative distance to the cloud explaining the observational corrugation in near spiral arms. The Perseus and Cygnus arms offset from the galactic plane in the second quadrant are caused by the corrugation of the galactic plane.

Non-uniformity of the spiral arm would cause an increase in uncertainty for gradient measurements. Non-uniformity occurs when the spiral arm tilts from parallel to the galactic plane. When the spiral arm tilts from the galactic plane, the lower temperature contour density width expands as we perceive more of the spiral arm. The net temperature change should stay at zero within the limits of the spiral arms. The difference in orientation might shift the contour density

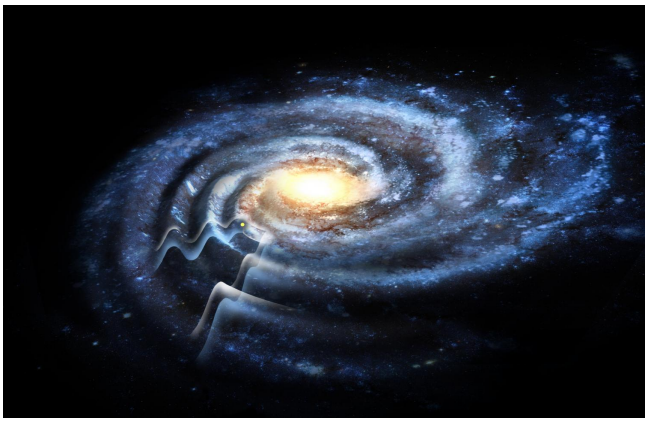

Figure 4: The corrugation image is from the Rensselaer Polytechnic Institute. The yellow dot represents our sun. An overlay of figure 1 can be traced over the corrugation image for all angles. The trace can be drawn in the second quadrant at a given latitude from the galactic plane.

peak location of the velocity-latitude pair resulting in increased uncertainty for gradient measurement of the spiral arm. Overall, any non-uniformity would cause a higher degree of randomness and scattering across the latitude length of the spiral arm and thus increase uncertainty in gradient measurements.

A bifurcation of the spiral arm would increase the uncertainty in a velocity measurement over the bifold. The bifurcation occurs when a section of the spiral arm splits into two distinct pieces depicted in figure 5. Gradient calculations using a Gaussian curve fit use the entirety of the velocity-latitude range of the bifurcation. A bifurcation is not always symmetric, shifting the Gaussian fit toward the higher density. Due to the splitting of the spiral arm, the measurement error will be relatively large.

The second quadrant is the most resilient to complications in measuring the rolling motion effect. In interior quadrants to the sun's position have overlapping hydrogen clouds along a line of sight. Figure 2 visually represents the data in all four quadrants and shows the characteristics of complications in the interior. In the second quadrant, minimal hydrogen overlap occurs when determining thermal contour density elevations. Figure 6 is an enhanced version of figure 2, which has distinct spiral arm features in the second quadrant. In figure 6, the CARS survey has the highest corresponding 1:1 ratio of thermal brightness to the hydrogen cloud latitude-velocity pair position. The second quadrant is the most resilient and best candidate to evaluate gradient measurements since it has the highest corresponding 1:1 ratio and the least number of complicating factors.

The crowding effect was observed in the first and fourth quadrant using figure 2. Multiple lines of tangents can be drawn from the spiral arms from the line of sight in the first and fourth quadrants. The crowding effect at the tangent

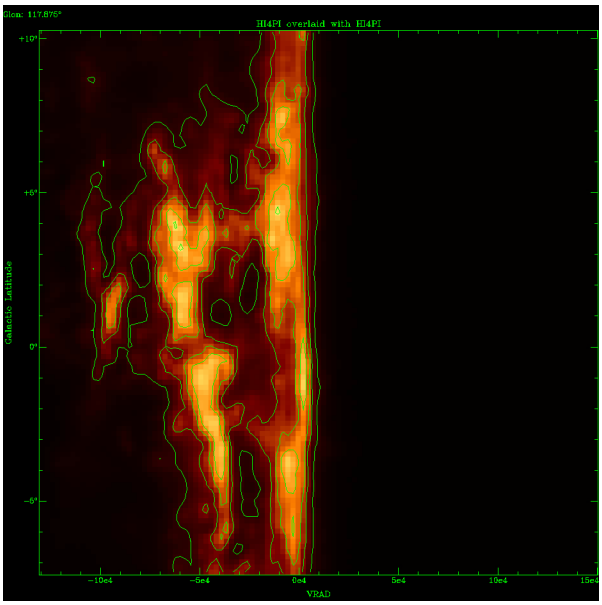

Figure 5: This image represents the bifurcation of the Cygnus arm. The bifurcation occurs around latitude of 5 degrees. The bifurcation of the Cygnus arm is present in the 50 percent contour mappings.

points from the line of sight increases the overlay of density. An accumulation of density overlay makes the first and fourth quadrant less accurate. The crowding effect causes an increase in uncertainty when demonstrating rolling motion.

The survey of the bridge between the second and third quadrant of the spiral arms changes the sign-in velocity. The Perseus and Cygnus arm contains deviation of the galactic plane with velocity values close to 0 m/s. Figure 7 displays the Perseus and Cygnus arms overlapping with the galactic plane density. The spatial positions of the spiral arms using contour map application determine gradient measurements. Figure 8 represents a contour map placed upon the velocity-latitude diagram with enhanced zoom. As the spiral arms transition from the second to the third quadrant, the thermal density will increase along the line of sight from the spiral arms and galactic plane. Contour density tracks the relative shift in velocity in the second quadrant as the spiral arms overlap with the galactic plane. Figure 9 depicts the velocity-latitude diagram of the spiral arms at a longitude of 166 degrees. Figure 9 represents the spiral arms approaching the galactic plane as they start to overlap in thermal density. Gaussian curve fits use velocity-latitude diagram's thermal density to measure the movement of the spiral arms in the second quadrant. Gaussian curve fits apply in the overlap region with the effect of increased density between the spiral arms and the galactic plane. As the spiral arms overlay with the galactic plane, the magnitude of the spiral arm and galactic plane density increases relative

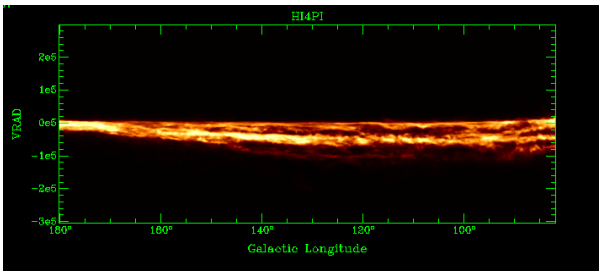

Figure 6: An enhanced version of figure 2, which presents a clear image of the second quadrant .

to that of the galactic plane. The tracking of the spiral arms throughout the second quadrant and the overlap of density against the galactic plane increases gradient measurement accuracy. The velocity-latitude positions in the overlap between the spiral arms and the galactic plane Are not measured using a different method than 20 and 50 percent of peak density fit. The latitude range applies to the overlap region in the second quadrant.

2 Data

2.1 Gaussian Fitting

The best approach to investigate the rolling motion phenomenon is to apply contour maps to velocity-latitude diagrams (Feitzinger and Spicker, 1985). Applications of contour maps to velocity-latitude diagrams are the most suitable approach for measuring rolling motion because of the clarity in determining the spiral arm structures. Contour maps use green outlines for every velocity-latitude diagram. These green outlines are lines of equal temperature and are used to determine the shape of the spiral arms. Velocity calculations use Gaussian curve fits to determine the velocity range of each spiral arm. The velocity range in a Gaussian measurement compares against each diagram. The Gaussian curve fits use every latitude measurement in the spiral arms to make velocity-latitude pairs. The resulting velocity-latitude position pair constructs a linear array to calculate the measured gradient.

Gaussian fitting over the distribution of latitudes is the best method to deal with measurement complications. Gaussian curve fitting is the most replicable and reliable determining source for gradient measurements. A velocity fitting complication arises when the spiral arm exhibits a tilt from the galactic plane. Gaussian curve fitting obtains fewer degrees of randomness and scattering when the spiral arm tilts. Measurements of velocity from the velocity-latitude diagram at a constant longitude would average across the tilt but could shift the velocity distribution. Gaussian curve fitting is the most accurate way of determining the gradient with a tilt since the distribution should be relatively

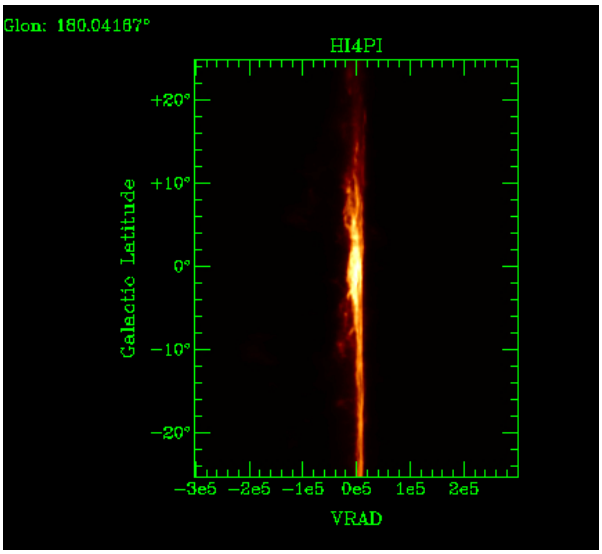

Figure 7: The CARS survey of the velocity-latitude diagram at a longitude of 180 degrees representing the sign change of velocity from the second and third quadrant.

symmetric. Another case for why Gaussian curve fitting is the best solution arises from the bifurcation of the spiral arm. The Gaussian curve fit will range over the entirety of the bifold, increasing the velocity range and determining the measured velocity between the split. The uncertainty in velocity measurement is significant in the case of bifurcation, but the Gaussian curve fits predict the most accurate velocity estimate from the distribution. The culminated point from the velocity-latitude temperature density diagram is not the resulting velocity from the Gaussian curve fit. Figure gamma shows the apex of the velocity data separated from the peak of the Gaussian curve fit. The minimization of the Gaussian curve fit obtains the velocity at each latitude for the centroid of the arm.

2.2 CARS Survey

Feitzinger and Spicker (1985) determine a new approach to the rolling motion using contour maps. Contour maps should have a small spacing in longitude and should be measured uninterruptedly. Small intervals of longitude from the CARS survey establish an array of velocity-latitude gradients over the entirety of the second quadrant. The CARS survey represents the best rolling motion calculations due to the highest possible spatial and velocity resolution currently available. Velocity measurements should contain the latitude range of the spiral arm, using as many velocity-latitude pairs available. The tracking process measures the spiral arms approaching the galactic plane within the second quadrant

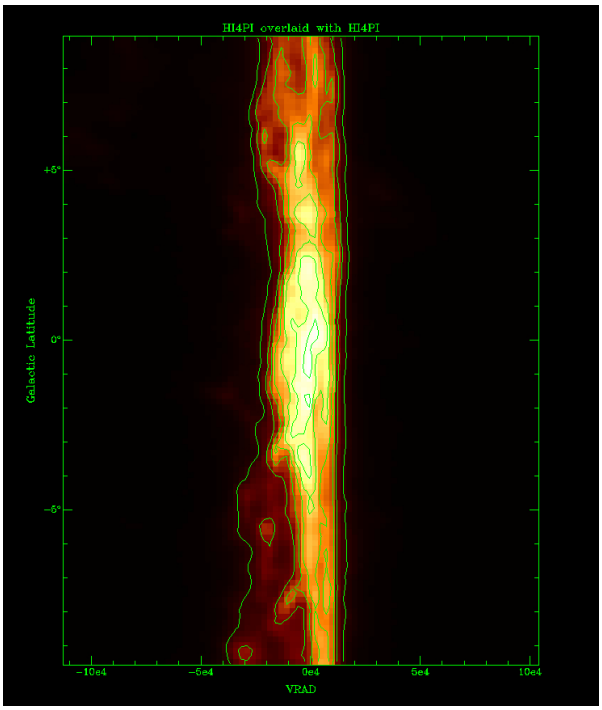

Figure 8: Applying a contour map to the CARS survey of the velocity-latitude diagram at a longitude of 180 degrees .

enhanced using smaller longitude intervals. The 0.65-degree latitude interval was chosen for the Perseus and Cygnus arms in the first and second quadrants to make sufficient velocity-latitude pairs required to determine the gradient. Due to multiple complications in the first quadrant, only the second quadrant is analyzed to evaluate rolling motion. The CARS 21 cm line survey of the milky way galaxy has high spatial resolution. The CARS survey displays resolution of the velocity-latitude diagram in a constant grid representation. The CARS survey for a velocity-latitude diagram has velocity resolution in intervals of 2576.4 m/s. The latitude and longitude resolution of the CARS survey is 1/6 of a degree. An intensity view of 99.99 percent was used to filter background sources of H1 and allow for the application of two different contour map levels. For a lower intensity view, the velocity-latitude diagrams would present a higher saturation of temperature density. For the best clarity in velocity-latitude diagrams a fire map was chosen for coloration with the highest possible intensity view.

2.3 Gradient Comparison

The contour map applied to the velocity-latitude diagrams has multiple layers of equal density. Figures presented in this study show the contour map applica-

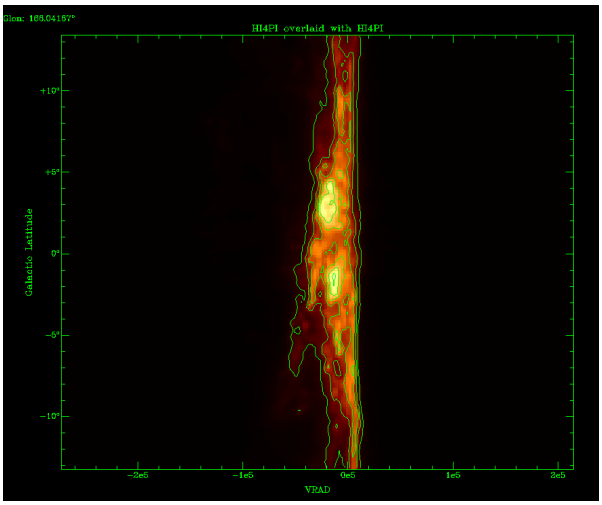

Figure 9: Applying a contour map of the velocity-latitude diagram to a longitude of 166 degrees. This visually represents the spiral arms converging with the galactic plane .

tion of [10,90] percent peak temperature density with an interval of 10 percent. The two different gradient measurements are 20 percent of peak density and 50 percent of peak density. The 20 percent contour map measures over an enlarged latitude range but allows for a greater velocity domain which causes increased scattering and randomness from the velocity distribution. The gradient measurement from 20 percent of peak density is the minimal requirement to have a proper filtration of temperature density with respect to velocity. Lower contours could contain a contribution from neighboring spiral arms and should not be used (Feitziner, J., Spicker, J., 1985). The 50 percent peak density test has a smaller latitude range and a smaller array of velocity-latitude position pairs with greater accuracy. The two contour levels determine gradients at longitude intervals of 10 degrees to determine if rolling motion occurs in the second quadrant.

Yuan and Wallace (1973) described the cross-section of the spiral arms in the Milky Way Galaxy to calculate theoretical gradients caused by the bending of the galactic plane. The points of tangency to a given density contour occur at the point where they intersect. The gradient of the spiral arms uses the tangent points to evaluate the linearity. A calculation of the mean Z scale of H1 was determined by the distribution of arm thickness along galactic longitude (Xinyu Du et al., 2016). The acquired mean Z scale of H1 resulted in 0.651 kpc used to evaluate all velocities along the galactic longitude in the second quadrant. Theoretical H1 calculation of the gradient uses the mean Z scale to compare gradients.

Theoretical velocity calculations adopted the modern constants to determine

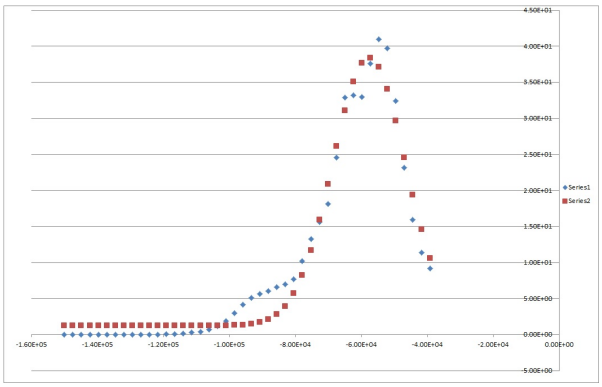

Figure 10: The Gaussian curve fit of a single velocity-latitude position pair. The blue diamonds represent the range of velocity for a given latitude. The red squares represent the Gaussian fit applied to the single velocity measurement. The Gaussian curve fit is restricted to velocities below the galactic plane such that the galactic plane does not influence the velocity fit.

the theoretical gradient. The modern constants are based on trigonometric parallax observation of star formation regions deriving R_o, $\frac{v_o}{R_o}$, and v_o. The modern constant values are R_o=8.40±0.6 kpc, $\frac{v_o}{R_o}$=30.65±0.9 $\frac{km}{s*kpc}$, and v_o=254 ±16 $\frac{km}{s}$ (Reid et al., 2009). The evaluation of the distance from the sun to the mean H1 distance was conducted using the collected Perseus and Cygnus fit of the second quadrant (Foster, Forster, 2021). Applying modern constants and mean Z scale leads to the most accurate current theoretical gradient measurements available.

Assumptions were made in the calculation of the theoretical gradient. Gradient calculation used the difference in the two tangent points of the mean Z scale of H1 throughout the second quadrant. The tangential velocity of the Perseus and Cygnus arm were measured using v=254$\frac{km}{s}$. All measured values for the Perseus and Cygnus arm fall within the modern constant value (Carignan et al., 2006). The average distance between the hydrogen cloud and the galactic center was calculated for the ten-degree interval to determine if the modern velocity is applicable to both the Perseus and Cygnus arms. The average radius was compared with measured tangential velocities to determine if v_o could be used for v. For both the Perseus and Cygnus arm the approximation of using v_o for v is within the error of v_o.

Rolling motion must occur in the Perseus and Cygnus arms to not be an apparent effect. The 20 percent and 50 percent gradient measurements with the theoretical gradient calculation should produce a 1:1 plot with no vertical shift if the rolling motion is an apparent effect. Rolling motion might not be an apparent effect if the slope measurement or vertical intercept were significantly different. Comparing gradient plots with intercept shift and forcing no intercept shift should be sufficient to determine if rolling motion occurs in the spiral arms.

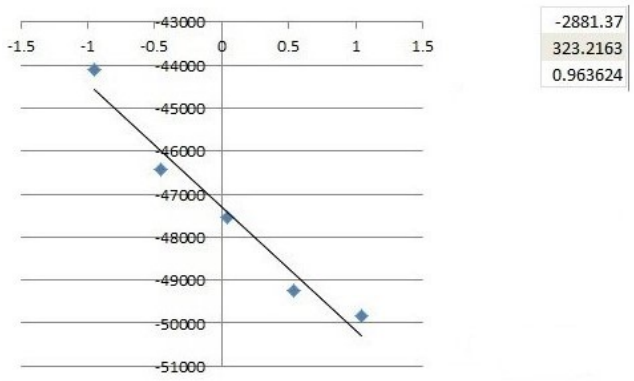

Figure 11: This image represents the velocity measurements acquired from Gaussian curve fits at the longitude of 130 degrees. The gradients of velocity-latitude measurements using Gaussian curve fitting is forced into a linear fit for the spiral arms. Each blue diamond represents the evaluated velocity at a given latitude for every latitude-velocity position pair. This linear fit of 20 percent of peak density proves the linearity of the gradients through all measured velocity-latitude position pairs.

Perseus Gradients						
longitude	20k gradient	δ20k	50k gradient	δ50k	20k theoretical	50k theoretical
90	-4176.564781	791.1444854	-4176.564781	791.1444854	-1347.599987	-1347.599987
100	-1120.416905	443.5960616	-1894.88092	860.5879103	-1048.367043	-1805.588602
110	-1404.134371	457.1634072	-2892.209625	1302.313599	-750.9893232	-1567.881181
120	-2350.559874	855.6541193	-3128.84506	1602.288813	-1013.199447	-1599.078407
130	-2881.366953	323.2163028	-3494.663162	684.9279467	-1960.788636	-3951.560713
140	-1114.771093	205.7757156	-1713.270363	581.9227383	-903.4880401	-1798.292263
150	-2122.050302	215.1251526	-1941.278754	317.6360993	-556.9518529	-1006.356596
160	-2537.208641	245.807802	-2191.830224	222.6444175	-621.0024714	-866.0482188
170	417.8402125	410.5408651	-165.7587585	331.7063429	-367.9951468	-438.9344581
180	1606.776613	410.1171927	1879.205036	578.5612066	-3.1179E-13	-3.87746E-13

Figure 12: The Perseus gradient table describes all measurements and theoretical calculations for gradients spanning the second quadrant.

For the second quadrant, the Perseus arm calculations of 20 percent and 50 percent were contradictory in the result. The 20 percent test resulted in Data=2.28 $\pm$0.720*Theoretical+389 $\pm$720$\frac{m}{s}$ with an R^2=0.557. The 50 percent test resulted in Data=1.08 $\pm$0.438*Theoretical-417 $\pm$769$\frac{m}{s}$ with an R^2=0.433. The 20 percent test suggests that real rolling motion occurs in the second quadrant, while the 50 percent test would suggest that the rolling motion could be fully apparent. The quality of the linear fit determined by R^2 implies that the 20 percent data would be more accurate. The quality of the 20 percent data is more susceptible to temperature influence which is not accounted for by the R^2 calculation. With contradictory results, a small rolling effect could potentially occur in the Perseus arm if no vertical shift is the better gradient evaluating method.

For the second quadrant, the Cygnus arm calculations of 20 percent and

Cygnus Gradients						
longitude	20k gradient	δ20k	50k gradient	δ50k	20k theoretical	50k theoretical
90	-6555.404924	1266.259186	-6555.404924	1266.259186	-2270.905471	-2270.905471
100	-2410.980572	1834.140311	-6134.538004	845.7115174	-899.8582169	-1283.02389
110	-2861.749741	395.2522697	-2719.440704	546.7608912	-1333.402442	-1333.402442
120	-835.3474446	328.7630367	-1758.053265	389.2310604	-860.6359221	-1013.599058
130	328.1916552	910.7465067	489.4651775	1687.8231	-2049.991846	-1543.495959
140	403.7123531	365.8059866	-1080.428171	417.7689841	-539.184095	-1346.280096
150	-1046.48106	408.5418546	-584.2907341	160.5309834	-334.1858684	-1124.871945
160	4.636741388	356.8572568	1577.170901	327.2788457	-371.6507468	-783.6748233
170	1266.407081	1715.564424	1387.829776	417.1021154	-165.8698733	-539.0483097
180	602.0868913	203.7437234	-629.6340944	315.5215278	-1.01677E-13	-2.80117E-13

Figure 13: The Cygnus gradient table describes all measurements and theoretical calculations for gradients spanning the second quadrant.

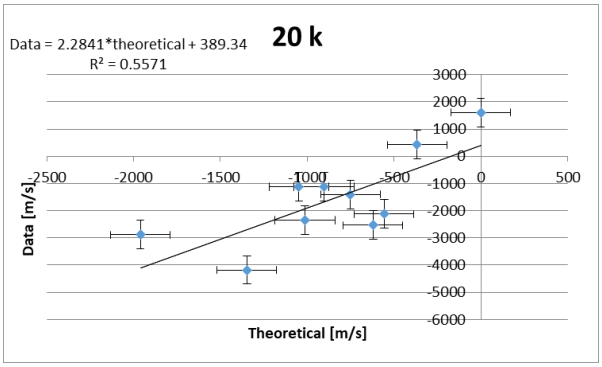

Figure 14: The Perseus linear fit of gradients using a 20 percent of peak plot in the second quadrant.

50 percent were both conclusive in the result. The 20 percent test resulted in Data=2.02 $\pm$0.777*Theoretical+671 $\pm$894$\frac{m}{s}$ with an R^2=0.458. The 50 percent test resulted in Data=2.86 $\pm$1.29*Theoretical+1610 $\pm$1630$\frac{m}{s}$ with an R^2=0.579. Both calculations showing a significant difference in the ratio between measured and theoretical gradients. These significant results show that rolling motion should occur in the Cygnus arm if no vertical shift was the better gradient evaluating method.

Forcing the gradient comparison through no vertical offset resulted in a higher average R^2. A higher average R^2 produces a more accurate linear fit. The Perseus arm with a forced linear fit compared against no vertical offset increased the average R^2 value by 0.268. The Cygnus arm with a forced linear fit compared with no vertical offset increased the average R^2 value by 0.093. Applying no vertical offset for linear fitting significantly tightened the gradient distribution. A direct comparison with no intercept shift between theoretical and measured gradients is more reliable than allowing for a vertical offset because of the increased average value. The 1:1 linear fit with no intercept offset better determines if rolling motion occurs in the spiral arms.

The linear fit of the Perseus arm using the 20 percent and 50 percent tests had similar results in the second quadrant. The 20 percent test resulted in

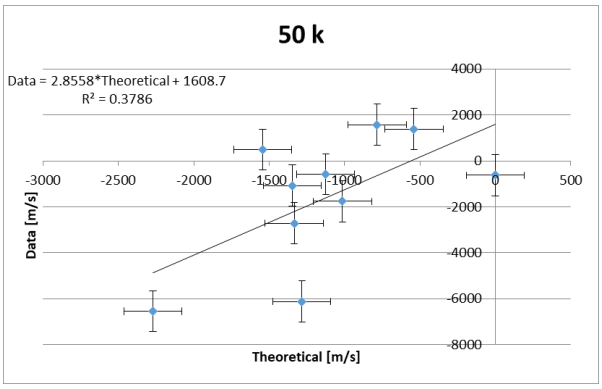

Figure 15: The Cygnus linear fit of gradients using a 50 percent of peak plot in the second quadrant.

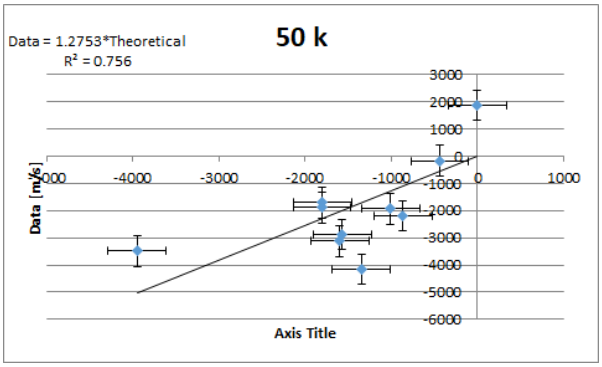

Figure 16: The Perseus linear fit of gradients using a 50 percent of peak plot in the second quadrant.

Data=1.95 $\pm$0.6556*Theoretical$\frac{m}{s}$ with an R^2=0.769. The 50 percent test resulted in Data=1.28 $\pm$0.242*Theoretical$\frac{m}{s}$ with an R^2=0.756. The 20 percent test suggests that there could be real rolling motion should occur in the second quadrant. The 50 percent test suggest that rolling motion could occur to a small degree.

Data=1.72 $\pm$0.591*Theoretical$\frac{m}{s}$ with an R^2=0.486. The 20 percent and 50 percent tests suggests that there could be small rolling motion in the second quadrant. The 20 percent and 50 percent contour mapping tests provide two different resources of gradient measurements. 50 percent contour measurements are more reliable since they are more resistant to other sources of temperature density. The 20 percent data is more susceptible to temperature density influence resulting in less reliable conclusions. Larger negative averages are observed in the Perseus and Cygnus arms and are measured using 20 percent and 50 percent contour tests compared to theoretical gradients. Density influence increases

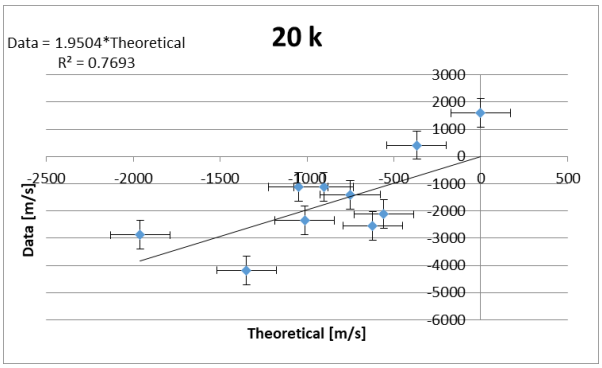

Figure 17: The Perseus linear fit of gradients using a 20 percent of peak plot in the second quadrant.

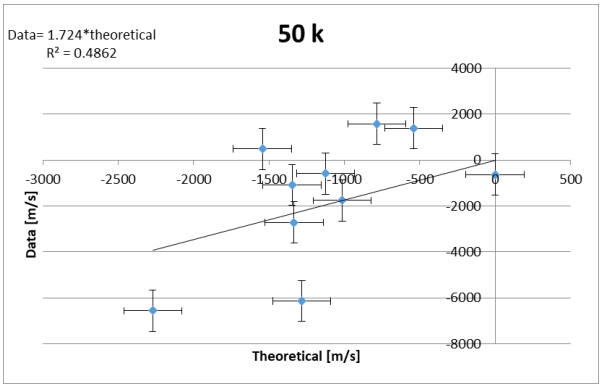

Figure 18: The Cygnus linear fit of gradients using a 50 percent of peak plot in the second quadrant.

the gradient error in magnitude measurements, which are more likely to influence the 20 percent test. The 50 percent gradient measurements have a reduced latitude domain resulting in significantly less density influence. Evidence for rolling motion must occur from every linear fit to be significant.

3 Results

For the rolling motion to not be an apparent effect caused by the combined effects of bending of the galactic plane and differential motion, uniformity of negative gradients across all measurements must occur. There must be a significant difference in the magnitude between the theoretical gradient and the measured gradients for rolling motion. If both conditions are satisfied, the rolling motion would exist.

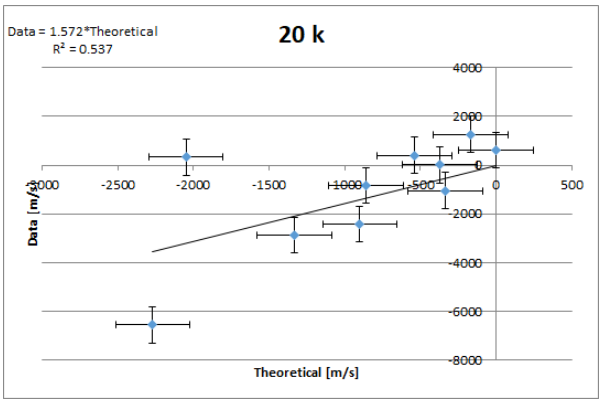

Figure 19: The Cygnus linear fit of gradients using a 20 percent of peak plot in the second quadrant.

Theoretical measurements for the Perseus and Cygnus arms are consistently negative within error agrees with Yuan and Wallace's predictions (1973). Yuan and Wallace concluded that the inner spiral arms do not have uniform negative gradients. The conclusion from my results using contour maps corresponds with Yuan and Wallace's gradients measurements. The apparent rolling motion they described appears where the plane is distorted, occurring between [20,140] degrees. All gradients measured in the distorted plane were always uniformly negative within error. Measurements in the plane's distortion result in a 1:1 relationship outside of error supporting that rolling motion is not only an apparent effect. The magnitude of the gradient was the largest within the distortion of the plane suggesting that the systematic rolling motion observed has some high correspondence with the bending of the galactic plane.

The gradient measurements of the Cygnus arm in the second quadrant are not uniformly negative in value but are mostly uniformly negative within error. The overall error range accounts for most of the positive gradient measurements. The gradient becomes positive in value for the Cygnus arm but is negative within error with the bifurcation in longitude of 130 degrees. Multiple gradient measurements were positive in the longitude range of [130,180] degrees. The tracking method and the overlap of spiral arms for 170 and 180 degrees were positive but will contain the most randomness and scattering. The gradient will also change sign passing from the second quadrant to the third at 180 degrees of galactic longitude. Valuations approximating zero within an error are reasonable. Strong evidence against the rolling motion is presented for the Cygnus arms if the gradients are not uniformly negative in the second quadrant. The longitude range of [90,140] degrees gradient measurements was uniformly negative supporting the theory made by Yuan and Wallace (1973). The longitude range [130,180] degrees contained positive gradient measurements that fell outside the error range. The gradient measurements are not uniformly negative over the second quadrant providing evidence against the rolling motion.

The gradient measurements of the Perseus arm in the second quadrant are consistently negative. Apart from the gradient measurement at 170 and 180 degrees, all other gradients were negative. 170 and 180 degree gradients had lower accuracy because of the overlap between the spiral arm and the galactic plane. Evidence is provided for rolling motion in the Perseus arm due to uniform negative gradients in the second quadrant. The Perseus gradients using 20 percent is twice the magnitude of theoretical measurements. Gradient measurements using the 50 percent test also suggest that the rolling motion is not an apparent effect. The magnitude disparity for the Perseus arm between the 20 percent and 50 percent test determines that the reliability of using the 20 percent test is lower than expected. The 20 percent and 50 percent contour tests represent a significant difference in temperature density. Both gradient measurements should agree within error and do not for the Perseus arm. The reliability of 20 percent measurements is mentioned in the discussion section.

4 Conclusion

The theoretical differential motion calculated and measurements using 20 percent and 50 percent contour map fall outside error. Gradient measurements were larger in magnitude than theoretical calculations. A significant average gradient difference between the measured and theoretical gradients occurred. Theoretical and measured gradients had a significant difference in every linear fit. Average calculations included positive gradient measurements for the Perseus and Cygnus arms in the second quadrant, which theoretically should not happen. Most measured gradients should have the same sign within error for their respective quadrants. The gradients for the Perseus arm are within error, excluding galactic longitude of 180 degrees. The Cygnus arm has positive gradients outside of error for galactic longitudes of 160 and 170 degrees using the 50 percent contour test. Uniformity of negative gradients occurred for every Perseus arm measurement, but the Cygnus arm did not have uniformity using the 50 percent contour test. The gradients from the CARS survey trended toward lower negative magnitude for the Perseus and Cygnus arms as they trend towards the galactic plane in the second quadrant. The negative gradient of the Perseus arm was significantly less than the Cygnus arm.

The no vertical intercept offset plot has a lower variance than the vertical intercept offset. All contour plots using the no vertical offset have a small amount of rolling motion that occurs in the second quadrant since a 1:1 linear fit fell outside of error. The linear fit using the 50 percent contour test resulted from the Cygnus arm having a significant difference in theoretical and measured gradients than the Perseus arm, suggested by Yuan and Wallace (1973). The CARS survey showcased a small rolling motion in the second quadrant that could not be explained by Yuan and Wallace (1973). The rolling motion observed in the second quadrant should translate to the other quadrants in the milky way galaxy.

5 Discussion

H1 clouds have variations in the valuation of surface temperature density (Xinyu Du et al., 2016). Colder and optically thick H1 gas could cause surface density variation. Cold and optically thick H1 gas has been observed in the outer parts of our galaxy and would distort the temperature density along a line of sight. When colder and optically thicker H1 clouds overlap, a change in the surface temperature density occurs. A noticeable shift in temperature would happen between the linear fits for 20 percent compared to 50 percent. The linear fits using a range under 20 percent would have the highest amount of this surface density variation. The 10 percent temperature density range is expansive in the velocity-latitude diagrams seen on figure 3. The colder and optically thicker H1 clouds could influence the gradient magnitudes measured using the gaussian curve fit and increase uncertainty.

An increasing trend of spiral arm thickness with respect to the galactocentric radius is accepted (Wouterloot et al., 1990; Kalberla, Kerp, 2009). H1 thickness of the spiral arms increases with relative distance to the galactic center. The Perseus arm has a thickness of 200, and the Cygnus arm has a thickness of 550 pc (Xinyu Du et al., 2016). Thickness measurements in the outer arm range between 400-600 pc (Sun et al. 2015). An overlap of H1 clouds within the spiral arms occurs with an increasing trend in the thickness of the spiral arm. The assembling of H1 clouds along a line of sight influences the temperature density in the spiral arms. The amount of equal density contour lines increases with the increasing trend of thickness visible within figure 3, as the Cygnus arm contains more equal density contour lines than the Perseus arm.

Hydrogen clouds are ellipses displaced along the spiral arms and can not be circular. A circle's orientation is unaffected when displaced above the plane. 20 is an exaggerated case of latitude shift from the galactic plane to a visual representation of the difference between a circle and an ellipse. An ellipse will change in orientation with respect to the galactic plane when tilted above the plane. If the hydrogen clouds were circular, we would expect the opposing sign in gradient measurement for the second quadrant. Circular gradient measurements would have a contradicting sign than observation of the hydrogen clouds. Hydrogen clouds are elongated along the trajectory of the spiral arm. Gradient measurements suggest that the hydrogen clouds are ellipses since the gradient sign corresponds with the representation predicted with an elliptical cloud.

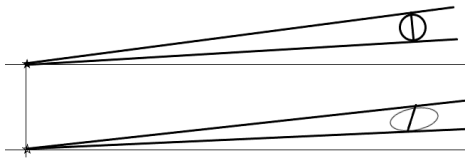

Figure 20: The comparison between a circle and an ellipse.

6 References

1. Claude Carignan, Laurent Chemin, Walter K. Huchtmeier, and Felix J. Lockman, 2006, 641:L108-L112

2. Feitziner, J., Spicker, J., 1985, MNRAS, 214, 539-558

3. Foster, Cooper, 2010, ASP

4. Foster, Forster, 2021, r mapping

5. Kalberla, P. M. W., Kerp, J. 2009, ARAA, 47,27

6. M. J. Reid, K. M. Menten, X. W. Zheng, A. Brunthaler, L. Moscadelli, Y. Xu, B. Zhang, M. Sato, M. Honma, T. Hirota, K. Hachisuka, Y. K. Choi, G. A. Moellenbrock, and A. Bartkiewicz, 2009, ApJ, 700:137-148

7. Rensselaer Polytechnic Institute, 2015, corrugation image

8. Sun, Y., Xu, Y., Yang, J., et al. 2015, ApJ, 798, L27

9. Wouterloot, J. G. A., Brand, J., Burton, W. B., Kwee, K. K. 1990, AA, 230, 21

10. Xinyu Du, Ye Xu, Ji Yang, Yan Sun, Facheng Li, Shaobo Zhang, and Xin Zhou, 2016, ApJ, 9

11. Yuan, Wallace, 1973, ApJ, 185, 453

12. Yan Xu, Heidi Jo Newberg, Jeffrey L. Carlin, Chao Liu, Licai Deng, Jing Li, Ralph Schönrich, Brian Yanny, 2015, ApJ